DOI: 10.1002/stco.202000031

Jörg Lange, Thilo Feucht, Maren Erven

3D printing with steel

Additive Manufacturing for connections and structures

Extended keynote paper of Eurosteel 2021

Automated production is finding its way into the fabrication of structural steel. One robot holds attachments (stiffeners, end plates, etc.) on a steel beam or column and another robot produces weld seams. However, welding robots can also be used for Additive Manufacturing (Wire and Arc Additive Manufacturing, WAAM). The wire electrode serves as a printing material. The Institute of Steel Construction and Materials Mechanics in Darmstadt is investigating how typical connecting elements for steel structures can be printed directly on steel beams using Additive Manufacturing with arc welding and robots. Furthermore, structural elements such as nodes for space frames can be printed and even complete structures, e.g. columns and a little bridge, have already been manufactured additively. The main focus is on determining suitable welding and process parameters. In addition, topology optimization is necessary in order to achieve good structures using a small amount of material. This is possible due to the free design prospects of WAAM, which opens up new design and production strategies.

Keywords Additive Manufacturing; WAAM; welding; topology optimization; connections; 3D printing

1 Introduction

The 3D printing technique is not yet fully established in the construction industry, which requires long-term reliability (an issue extremely important for buildings with an expected lifespan of 50–100 years), low costs for construction coupled with the limited development in manual skills due to low wages and the industry's poor reputation. However, by understanding the potential for individualization and automation, a clear trend towards applications for 3D printing can be identified in building technology and construction [1].

The technologies of 3D printing, which is also called "Additive Manufacturing" (AM), are progressing rapidly. The printing materials are manifold and printing on and with steel is now also easily possible. In Additive Manufacturing, a component is created by adding material, unlike milling, which removes material from a structural part. Selective Laser Melting and Selective Laser Sintering are available for the Additive Manufacturing of steel. Another method is Laser Metal Deposition, in which a metal powder is applied to a local molten pool generated by the laser [2, 3]. All these methods are highly accurate, but also entail high equipment and material costs. Furthermore, they have low deposition rates and a small construction space, since the powder has to be kept in a closed cell.

Wire and Arc Additive Manufacturing (WAAM) [4], which is similar to Gas-Shielded Metal Arc Welding (GMAW), is suitable for steel construction. The wire electrode serves as a printing material. Using this method it is possible to produce large components in layers (see Fig. 1), with nearly no size restrictions and achieving deposition rates exceeding 5 kg/h [5, 6]. With such rates, the application will be more successful commercially in the field of connections and joining technology rather than the fabrication of complete structures.

Additive Manufacturing in general and the welding process WAAM in particular allow a more targeted use of the material than in the past. Structures can be freely modelled and be almost any shape. Unlike conventional steel construction using plates and I-sections, AM-based production hardly limits the form of construction. The customary trade-off between cost-effective production and material-savings is unnecessary. Material only needs to be placed where it is required. Therefore, it is expedient to develop these structures using topology optimization, which leads not only to reduced material consumption, but also shorter production times.

In addition, AM can be used to improve production chains, e.g. by avoiding delivery times for spare parts or by

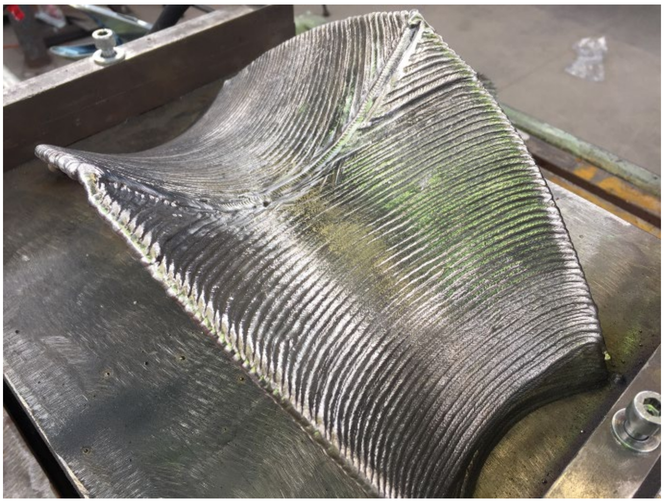

(© Benedikt Waldschmitt)

Fig. 1 A structure additively manufactured using WAAM simplifying logistics in general. Currently, only a few fully automated I-beam assemblers [7] are used in steel fabrication companies worldwide. In these machines, handling robots hold plates (stiffeners, end plates, etc.) while welding robots produce the welds. With AM, the logistics of these plates can be avoided. It is no longer necessary to stock different plate thicknesses for small numbers of plates, because the stiffener is printed directly on the I-section. Furthermore, it is easily possible to take deviations in the flange alignment into account. If the flanges are not parallel, this might lead to fitting problems with prefabricated plates. With AM, the stiffener is printed exactly in place, thus allowing for any possible deviations.

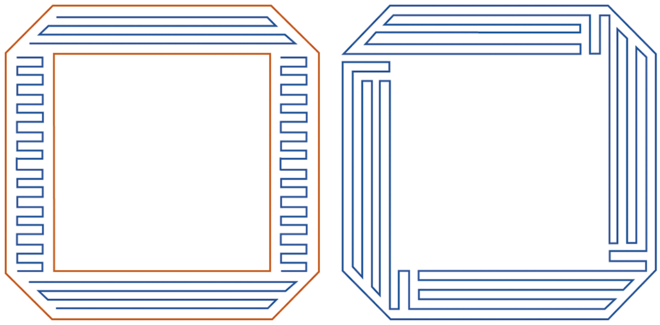

Fig. 2 Two different strategies for manufacturing a layer [7]

2 Influences on geometry and material properties

2.1 Slicing

Slicing is the process of partitioning the final geometry into layers or dots onto which the material has to be deposited. The layers are described by movement commands (mostly linear or circular) for the print head (the welding gun) and coordinates. Conventional 3D printers usually use the so-called G-code, which is also commonly used for machine control. Existing slicing software generates the layers and the G-code for common printers automatically.

Depending on the final geometry, various options and slicing strategies are possible, see Fig. 2.

For conventional and commercially available 3D printers, parameter sets exist which allow almost any geometry to be printed without the need for any investigations. Slicer programs divide a 3D body into paths along which the print head travels at a corresponding speed, applying the material in such a way that the planned structure is created.

Various parameter investigations already exist for WAAM. They cover a very wide range of materials (mild steel, stainless steel, aluminium, titanium, alloys) and production equipment (power source, robotics), but cannot be applied in all cases. The parameters required might become complicated for complex multilayer geometries. It is therefore essential to gain a better understanding of all parameters. This becomes more obvious when looking at the many influences on the geometry and the material properties, and thus the slicing algorithms.

The material deposition of WAAM and conventional 3D printers using plastic filaments is alike and leads to small beads, as can be seen in Fig. 1. However, filler wire has a far lower viscosity than common 3D printer filaments made from thermoplastic polymers (mostly polylactides, PLA), thus increasing the problem of producing a stable geometry. The magnitude of the viscosity, the cooling velocity and therefore the solidification of the molten metal are critical for the geometry and the material characteristics of the weld seam. The factors that influence the geometry and the material characteristics are manifold and are listed below. If these parameters are not well adjusted, the molten steel will not harden and stay at its destination, instead drip and flow somewhere else. This might prevent the production of overhanging structures.

2.2 Input parameters

- Wire electrode
- Wire diameter
- Shielding gas
- Gas flow rate
- Geometry of the gas nozzle
- Welding system

2.3 Process parameters

- Current
- Voltage
- Wire feed speed
- Welding process regulation (standard, pulse, CMT)
- Travelling speed

2.4 Thermal boundary conditions

- Interpass temperature
- Temperature history, temperature cycles
- Cooling

2.5 Geometric boundary conditions

- Orientation of the nozzle (neutral, dragging, piercing)
- Welding position (trough position, rising, falling)
- Contact tip to work distance
- Weld seam beginning, weld seam centre, weld seam end

3 Topology optimization

The optimization of a mechanical structure is called structural optimization. Three common categories of

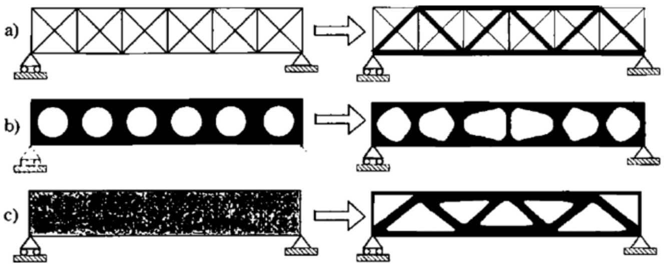

Fig. 3 Different types of structural optimization [9]

structural optimization are sizing, shape optimization and topology optimization (see Fig. 3). Sizing is the variation of numerical values, such as the cross-section of beams (see Fig. 3a). This principle is the foundation of each structural design. If the cross-sections are changed not only in size but also in shape over the length, this is called shape optimization (see Fig. 3b). In topology optimization, additional voids are inserted for unused, material-wasting areas of the structure (see Fig. 3c) [9] .

3.1 Definition of the solution method

Topology optimization can be divided into two types: mathematical topology optimization and empirical topology optimization [9]. The following investigations made use of mathematical topology optimization. The optimization problem was solved using the density distribution of the structure, which can be implemented with different approaches. The SIMP (solid isotropic material with penalization) approach is a simplification that assigns only one variable x to each element i. This variable x_i is the ratio of the momentary density ρ_i to the initial density $\rho_i{}^0$, see Eq. (1). The relation of the modulus of elasticity E of each element can be given by the power approach, see Eq. (2).

$$x_i = \frac{\rho_i}{\rho_i^0} \quad (1)$$

$$\frac{E_i}{E_i^0} = x_i^p \quad (2)$$

A p value > 1 should be considered in Eq. (2). Since topology optimization involves the formation of void, which are expressed by the modulus of elasticity E_i at these points (which are very small in comparison to the normal modulus of elasticity at fixed points $E_i{}^0$), a bigger exponent p leads to sharper designs than a small one. However, the computational effort is also greater in this case. The p value is also called the “penalty factor”, since it specifies how strongly a small density is “penalized”. A penalty factor of 3 was chosen in this investigation (see 4.4 and 4.5) [9].

3.2 Minimization of the mean compliance

The mean compliance C describes the sum of the work caused by the element displacement $F_i \cdot u_i$ over all the elements of the component, see Eq. (3). It provides conclusions about the stiffness of the component and therefore finding the minimum compliance is a suitable target function for the topology optimization of structural elements [10].

$$C = \sum_i \vec{F}_i^{\,T} \cdot u_i \quad (3)$$

It is logical that maximum stiffness is achieved if the volume V remains the same and is not reduced. However, this trivial solution has no practical benefit, as the component would remain the same and no material-saving design would result. Therefore, a volume restriction (Eq. (4)) is introduced. This means that, for a certain proportion v of the initial volume V_0, the minimum compliance must be found.

$$V - v \cdot V_0 \leq 0 \quad (4)$$

3.3 Implementation

When using topology optimization for structural design, one essential aspect must be taken into account. The algorithms currently in use cannot represent non-linearity. Therefore, it is not possible to consider plasticity, stability problems or non-linear bearings. In addition, it should be noted that the result of one optimization only gives the stiffest structure, but not whether the output can withstand the load. A subsequent non-linear analysis of the resulting structure is therefore always necessary.

The optimization described in section 4 was carried out using Ansys Workbench; the workflow is shown in Fig. 4. At first, the non-linear initial system was modelled realistically. The boundary conditions thus defined were transferred to the linear system. The linear system was then optimized for different mass ratios. The payload of each

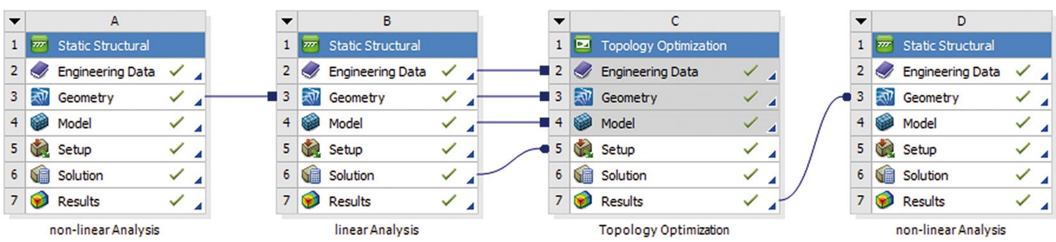

Fig. 4 Optimization workflow for one mass restriction

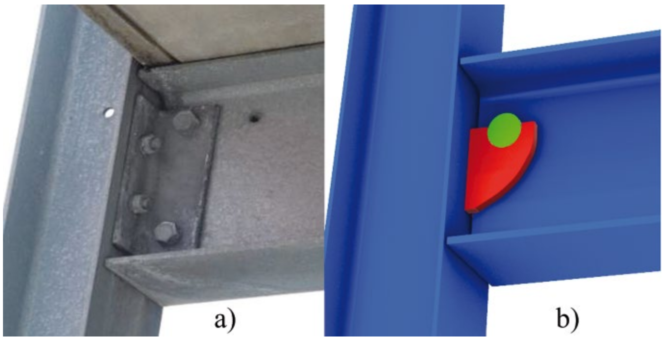

Fig. 5 a) Double angle connection, b) beam hook

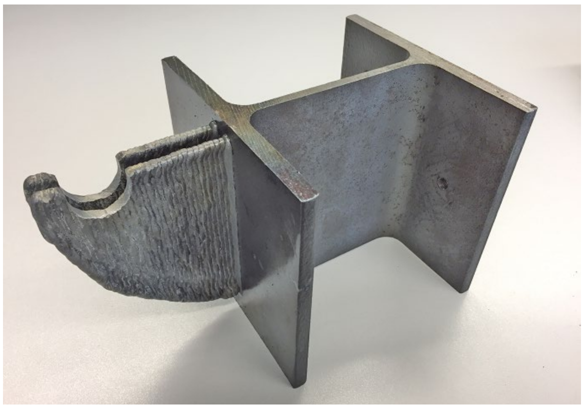

Fig. 6 AM-fabricated hook

optimized structure was determined in a subsequent nonlinear analysis.

4 Applications

WAAM has a high potential for applications in the field of connections, where little material is needed and this material might be subjected to great geometrical variation [11]. Furthermore, wherever great savings in material due to topology optimization are possible, WAAM will play an important role.

4.1 Beam hook

Connections between beams and columns are often designed as flag plates or with double angles, as shown in Fig. 5a. WAAM allows the production of a topology-optimized hook that transfers the load from the beam to the column via bolts (see Fig. 5b and Fig. 6) that could be printed on the web of the beam. The hook can be printed directly onto the column during fabrication. Erection is simplified as there are no nuts to be tightened.

4.2 Stiffener

Stiffeners are often used for better load transfer to an I-section and to prevent the flange from bending or buckling. Fig. 7 shows the printing of a stiffener.

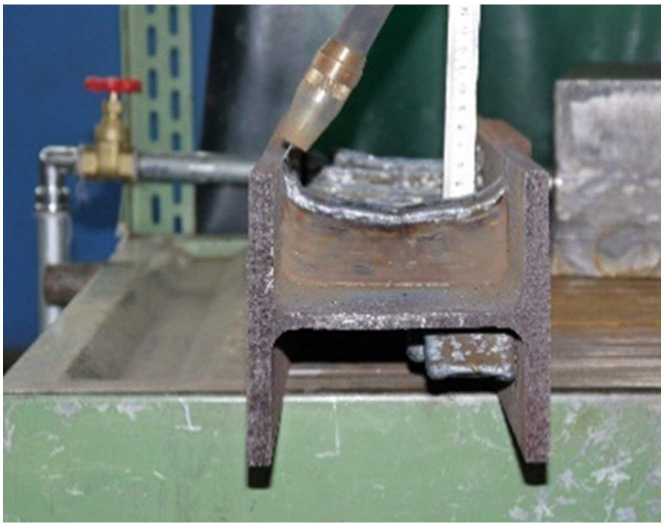

Fig. 7 Production of a stiffener

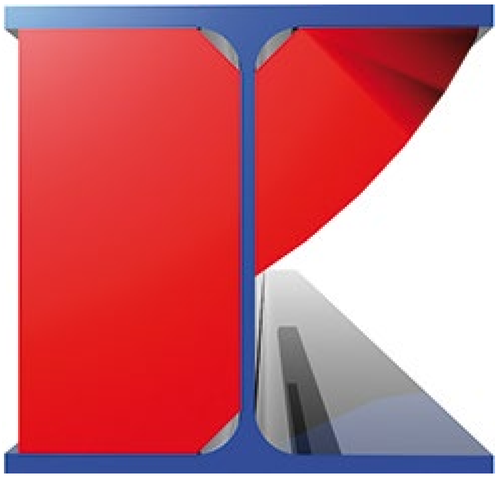

Fig. 8 Stiffener optimization

Since the angle of the welding gun can be changed, a continuous connection with the flange is achieved. Owing to the rolling tolerances, this is a great advantage over conventional stiffener plates, which might have to be machined. If the flanges are not quite parallel, the pre-cut plate might otherwise not fit. In traditional production, unloaded areas will not be removed (Fig. 8, left), as this would require additional effort and the waste is not usable. AM enables a reduction in size to reduce the material consumption. Every gram of steel needs valuable printing time. This leads to less material (Fig. 8, right).

4.3 Clamping elements for diagonal bracing

For common storage buildings, a clamping element is available which allows the very simple erection of diagonal bracing members. A half-moon-shaped element made of cast steel facilitates the installation of the bracing tie at nearly every possible angle (Fig. 9a). However, a curved adapter piece is also needed. With computer-aided design, the angle is known exactly and therefore a

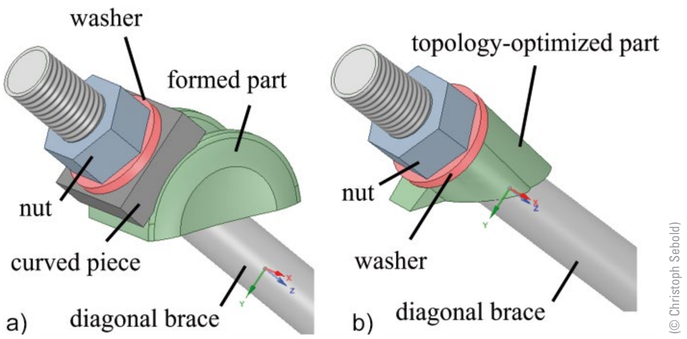

Fig. 9 a) Conventional clamping element, b) element optimized for AM

Fig. 10 Additively manufactured clamping element

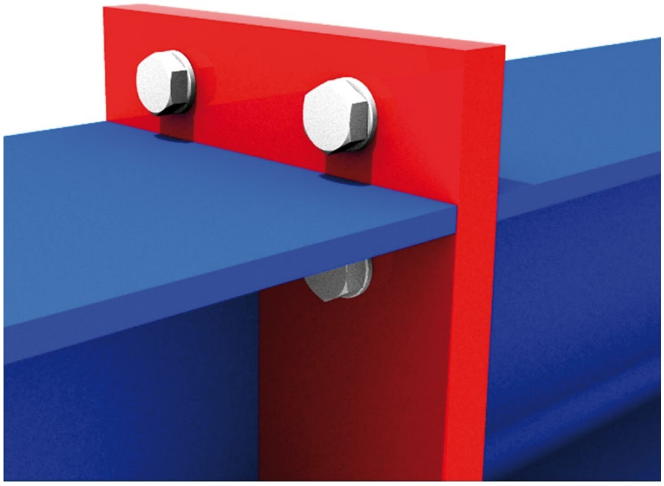

Fig. 11 Conventional T-stub end plate

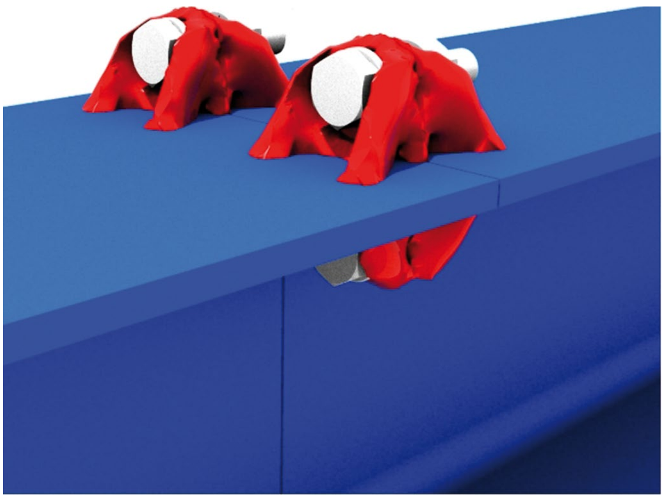

Fig. 12 Topology-optimized T-stub end plate

topology-optimized part can be printed onto the web (Fig. 9b and Fig. 10). This can be used together with a customary washer.

4.4 End plate replacement

In the case of rigid connections with end plates, moment and tensile force are transmitted with an eccentricity, since the bolted connection is not at flange level (see Fig. 11). The tensile force is transmitted from the flange to the bolt via bending in the end plate. To transfer this bending moment, the end plate normally needs to be very thick. Conventionally, this is designed by using a T-stub model. Taking into account the potentials of Additive Manufacturing, the geometry can be changed in such a way that efficiency improves and less material has to be used (see Fig. 12). The form-finding via topology optimization can be followed in Fig. 13. The T-stub for one row of bolts of the original plate has a loadbearing capacity of nearly 250 kN (red line). For optimization purposes, the design space was enlarged and restricted to at least the mass needed for a T-stub.

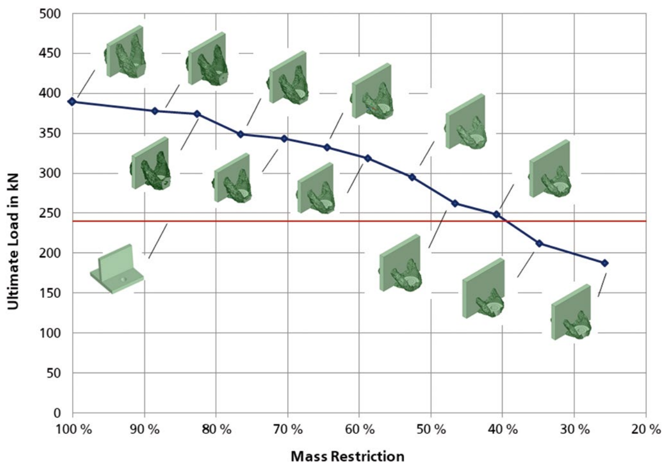

Fig. 13 Loadbearing capacity of different mass restrictions (blue) compared with the original T-stub design (red)

For different topology optimization results, the loadbearing capacity can be found on the blue line.

With the same mass as the T-stub, a structure results which has a loadbearing capacity more than 60% higher (nearly

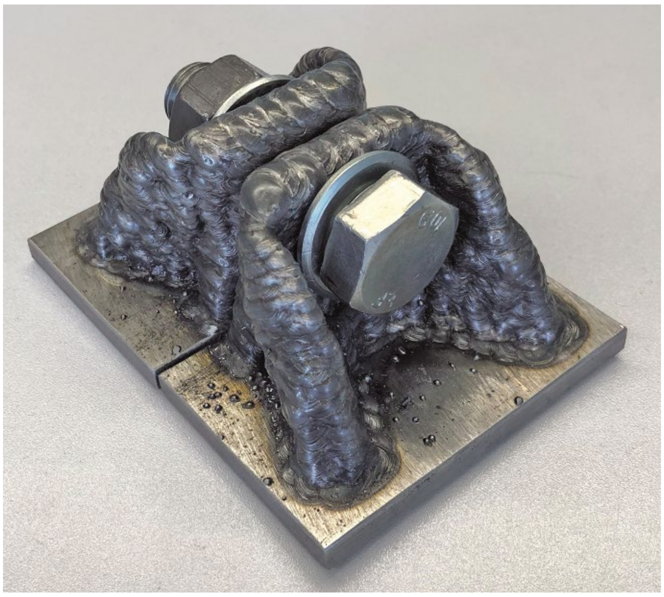

Fig. 14 WAAM-printed connection

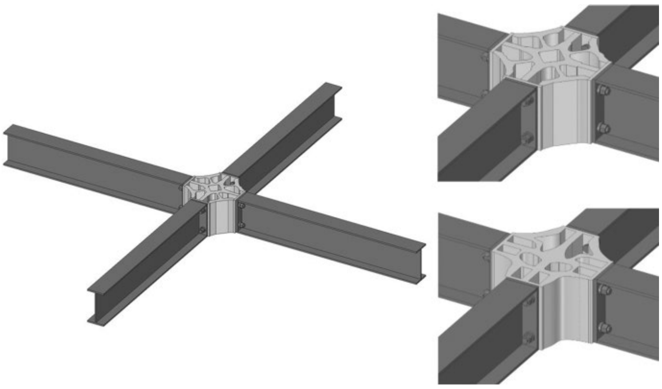

Fig. 15 Nodes in a space frame

400 kN). Furthermore, only 40% of the mass is needed to reach the same loadbearing capacity. This good efficiency can be traced back to the formation of “tension arms”. Thus, a longer “tension arm” transfers the eccentric force. A direct comparison with the conventional end plate reveals that the optimized connection is much lighter (see Fig. 11 and Fig. 12). In a follow-up study it was shown that WAAM is a suitable process for this new type of connection (see Fig. 14).

4.5 Node for space frame

Nodes can be defined as connecting points between steel members such as beams, girders and columns. Fabrication and erection should be simple and cost-efficient. Therefore, designers tend to create details that might use considerable material in order to reduce complexity in fabrication and erection. With the help of Additive Manufacturing, nodes could be custom-designed to suit the load case(s) and the geometry of the members to be connected. Structures can be designed according to the flow of forces using topology optimization methods. This

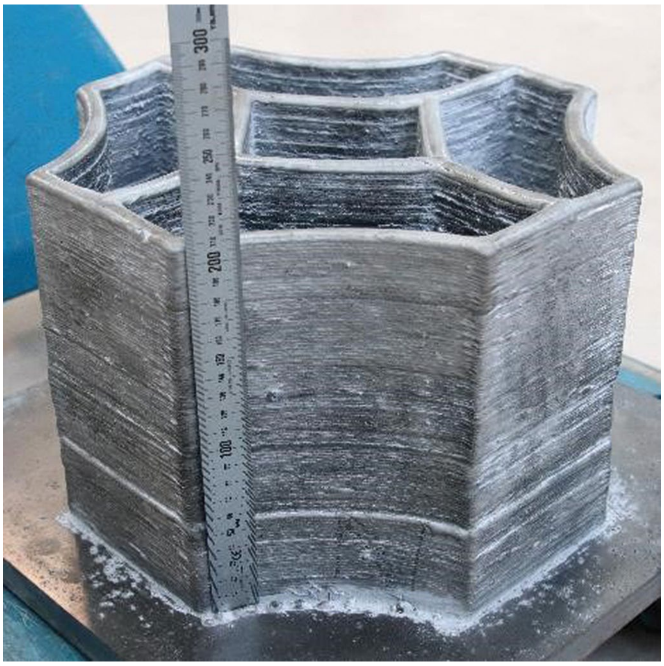

(© TU Ilmenau)

Fig. 16 Node for connecting four members

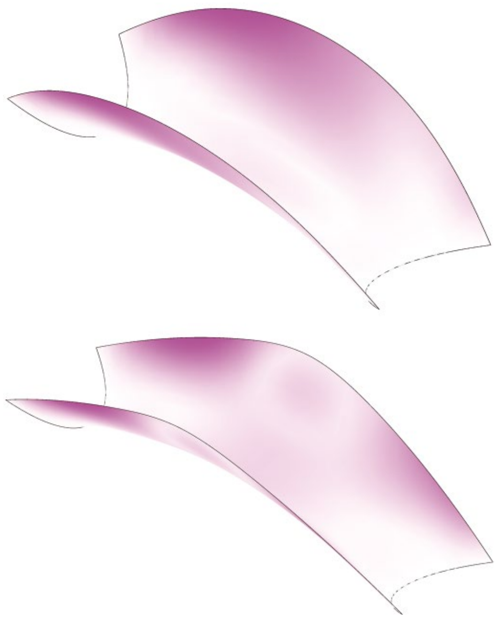

(© Christopher Borg Costanzi)

Fig. 17 Best designs according to Octopus

avoids material in places where it is not needed. Fig. 15 shows two examples for connecting four beams in a common plane but with different loads – symmetrical at top right, asymmetrical at bottom right.

With regard to WAAM, it must be kept in mind that small overhanging seams can be printed but that it is difficult and reduces the output (in kg/h) if vertical printing descends for more than 30°. This must be considered in all optimization procedures. Therefore, extruded, wall-like structures are very well suited to this process. Areas where seams meet or cross over each other might be challenging. Double-deposition will lead to distortion, other approaches can lead to voids or incomplete fusion.

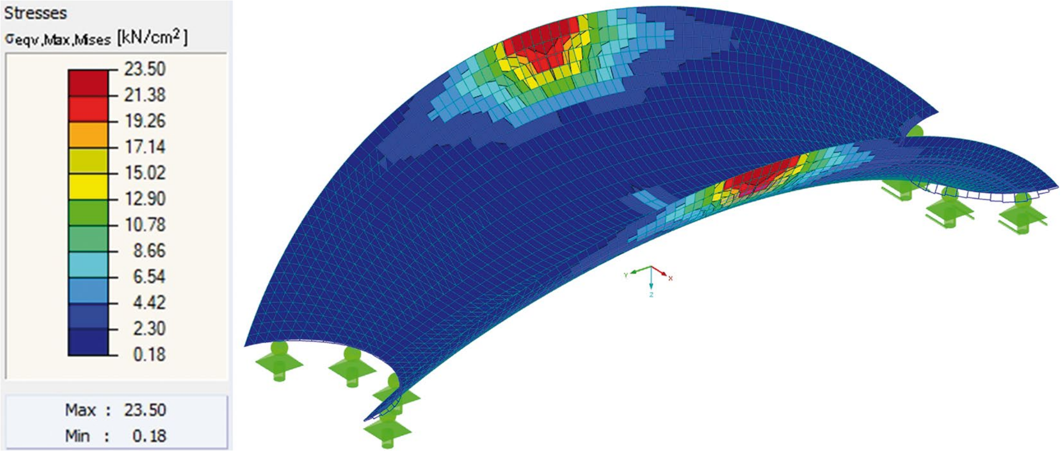

Fig. 18 Von Mises stresses in the model

Fig. 16 shows an additively manufactured node for connecting four members with symmetric loading. The holes for the bolts (connected via end plates) will be drilled conventionally.

4.6 AM bridge

In September and October 2019, a complete bridge spanning a little creek was printed in Darmstadt. Contrary to the well-known bridge of MX3D [12], this bridge was printed on site. Some challenges had to be met to solve this task:

- While printing horizontally, the molten steel tends to drip off the weld pool [13].
- A structure had to be designed that has enough strength to bridge the creek with a thickness that is optimally welded in one operation (approx. 5 mm).
- The material strength of the horizontally fabricated structure had to be good enough to carry the design loads.

The form-finding process for the bridge was performed with the Rhinoceros 3D software plus the Grasshopper 3D plug-in for parametric modelling and Karamba3D in combination with Octopus for form-finding. This allowed the bridge geometry to be quickly adapted to different site and loading conditions. With the help of Octopus, an evolutionary solver in Grasshopper 3D, a number of design options were generated with the following objectives: minimization of the elastic deformation energy and deflection under dead weight and minimization of the surface area and thus the total weight. It was therefore a multi-objective optimization problem.

The design options were additionally subjected to the following restrictions, which take into account the robot's reach, the width of the body of water to be bridged and the necessary accessibility. The total length of the bridge is between 2500 and 2800 mm, the entrance area has a width of 900–1100 mm and the width of the structure had to be kept within 1500 mm.

Taking these limitations into account, Octopus produced a point cloud with the best designs in relation to the set objectives. The two designs given in Fig. 17, selected from a large number of possible solutions, meet the aforementioned requirements. The final shape of the bridge was chosen on the basis of these proposals from an aesthetic point of view.

The structural analysis of the final design was carried out with the RFEM program from Dlubal. For this purpose, shell elements were used. A load of 5 kN/m^2 was applied. In addition, individual loads of 1.5 kN were applied at different locations in order to assess the effects of local

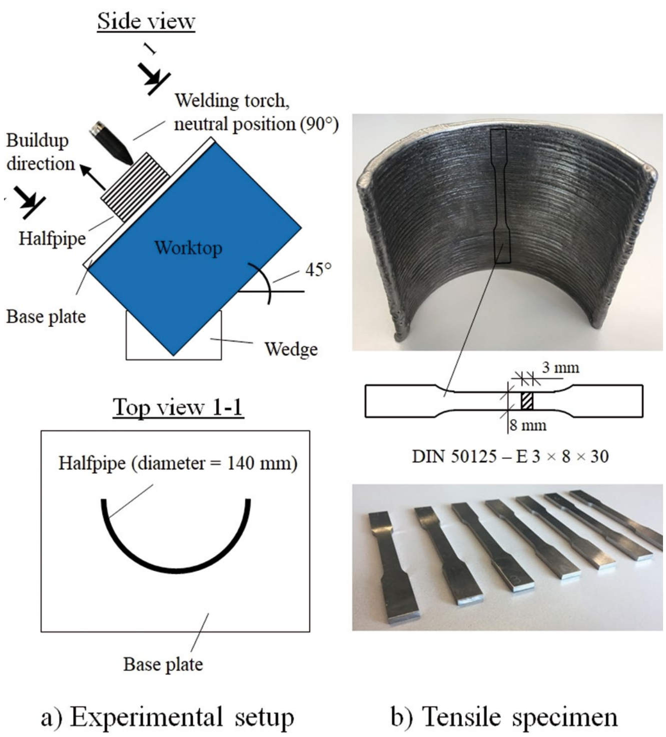

Fig. 19 Test setup and specimen

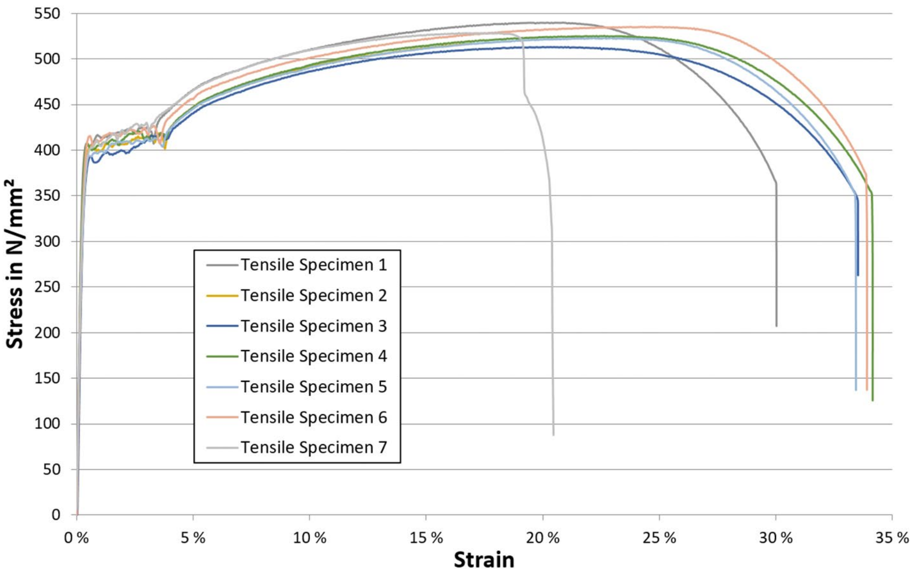

Fig. 20 Tensile tests

Fig. 21 Construction site

loads. Fig. 18 shows the von Mises stresses for the combination of uniformly distributed load plus two individual loads at the centre points of the edge lines (worst case).

During the development of the production process, a weld seam width of 6 mm was aimed for. However, in order to meet the manufacturing tolerances, e.g. due to a transverse offset of the welding positions or robot inaccuracies, a thickness of only 4.5 mm was used for the calculations.

To determine the strength of the cantilevered printed steel, a semi-tubular test specimen was manufactured at a 45° angle using CMT [14, 15]. Mild steel (G3Si1/ER70-S6) and a shielding gas with 82 % argon + 18 % carbon dioxide were used. Seven flat samples (3 × 8 mm) were milled out along the build-up direction. The test setup, the test specimen and the tensile specimens are shown in Fig. 19.

The results of the tensile tests are shown in Fig. 20. The yield strength has an average value of 403.0 N/mm^2 and a standard deviation of 7.4 N/mm^2. The manufacturer of the welding material gives the yield strength as at least 420 N/mm^2. This slight undercutting of the tensile test specimens is common in Additive Manufacturing, see [16]. The strengths are usually higher in tensile specimens that are loaded longitudinally to the course of the layers, so the unfavourable direction was assessed here. Studies involving other materials (e.g. stainless steel) can be found in [17, 18].

In addition to the preliminary investigation of the strengths, a model of the bridge at a scale of 1:8 was produced under controlled conditions in the laboratory (see Fig. 1). The advantage of the easy scalability of the parameterized object was used. The knowledge gained was used to produce the bridge. More information about the manufacturing parameters can be found in [19].

Fig. 22 The bridge after closure of the span

For the start of construction, the welding robot with controller, welding equipment, gas and wire was positioned directly on the side of a little creek on the TU Darmstadt campus. In order to protect unwary passers-by from looking into the arc on the one hand and to ensure the undisturbed flow of protective gas on the other, the construction site was enclosed in a tent. Founded on two base plates anchored in the ground, the bridge was printed in layers (see Fig. 21). The two cantilevers touched each other at the end of October 2019 (Fig. 22). As the construction site had to be cleared to make room for a new building and since the bridge had to be exhibited at a trade fair, the strips on the sides were not completely built up on site.

5 Conclusions

WAAM has a high potential for changing the production process in steel fabrication. Fully automatic fabrication machines using handling and welding robots will be able to print parts of structures in addition to welding ordinary seams. Up to now, some traditional connections have been redesigned and printed incorporating the advantages of Additive Manufacturing. This leads to valuable material-savings. Furthermore, new connection details for nodes in space structures were developed and, finally, a whole bridge was built, the first bridge printed in situ!

Acknowledgements

We would like to thank Chris Borg Costanzi as a part of our “AM Bridge 2019” team. We appreciate his advice and active support in every AM aspect. We also would like to thank the Fronius Deutschland GmbH, Messer Group GmbH, WDI Schweißtechnik GmbH, Comau Deutschland GmbH and Spinnanker GmbH companies for their kind support.

Open access funding enabled and organized by Projekt DEAL.

References

[1] Buchanan, C.; Gardner, L. (2019) *Metal 3D printing in construction: a review of methods, research, applications, opportunities and challenges* in: Engineering Structures 180, 2, pp. 332–348.
[2] Schmidt, T. (2016) *Potentialbewertung generativer Fertigungsverfahren für Leichtbauteile*. Berlin: Springer.
[3] Gebhardt, A. (2016) *Additive Fertigungsverfahren: Additive Manufacturing und 3D-Drucken für Prototyping – Tooling – Produktion*. Munich: Carl Hanser.
[4] Williams, S. W.; Martina, F.; Addison, A. C.; Ding, J.; Pardal, G.; Colegrove, P. (2016) *Wire + Arc Additive Manufacturing* in: Materials Science and Technology 32, 7, pp. 641–647.
[5] Almeida, P. M. S. (2012) *Process Control and Development in Wire and Arc Additive Manufacturing* [PhD Thesis]. Cranfield University School of Applied Sciences.
[6] Hartke, M.; Günther, K.; Bergmann, J. P. (2014) *Untersuchung zur geregelten, energiereduzierten Kurzlichtbogentechnik als generatives Fertigungsverfahren*, DVS report 306, pp. 31–35.
[7] Fischer, R. (2014) *Eine Untersuchung zur roboterbasierten Baugruppenfertigung im Stahlbau* [PhD Thesis]. Technical University of Darmstadt.
[8] Ding, D.; Pan, Z.; Cuiuri, D.; Li, H. (2014) *A tool-path generation strategy for wire and arc additive manufacturing* in: International Journal of Advanced Manufacturing Technology 73, 1–4, pp. 173–183.
[9] Harzheim, L. (2014) *Strukturoptimierung, Grundlagen und Anwendungen*. Haan-Gruiten: Verlag Europa-Lehrmittel.
[10] Bendsoe, M. P.; Sigmund, O. (2004) *Topology optimization: theory, methods, and applications*. Berlin: Springer.
[11] Feucht, T.; Lange, J.; Erven, M. (2019) *3-D-Printing with Steel: Additive Manufacturing of Connection Elements and Beam Reinforcements*, ce/papers Nordic Steel 2019 (Copenhagen) 3, 3–4, pp. 343–348.
[12] MX3D: https://mx3d.com/, access date: 17 June 2020.
[13] Yuan, L.; Ding, D.; Pan, Z.; Yu, Z.; Wu, B.; van Duin, S.; Li, H.; Li, W. (2020) *Application of Multidirectional Robotic Wire Arc Additive Manufacturing Process for the Fabrication of Complex Metallic Parts* in: IEEE Transactions on Industrial Informatics 16, 1, pp. 454–464.
[14] Posch, G.; Chladil, K.; Chladil, H. (2017) *Material properties of CMT – metal additive manufactured duplex stainless steel blade-like geometries* in: Welding in the World 61, 5, pp. 873–882.
[15] Fronius, Bruckner J.; Egerland, S.; Himmelbauer, K.; Millinger, A.; Schörghuber, M.; Söllinger, D.; Waldhör, A. (2013) *Schweißpraxis aktuell: CMT-Technologie. Cold Metal Transfer – ein neuer Metall-Schutzgas-Schweißprozess*. Kissing: WEKA MEDIA GmbH & Co. KG.
[16] Müller, J.; Grabowski, M.; Müller, C.; Hensel, J.; Unglaub, J.; Thiele, K.; Kloft, H.; Dilger, K. (2019) *Design and Parameter Identification of Wire and Arc Additively Manufactured (WAAM) Steel Bars for Use in Construction* in: Metals 2019, 9, 725.
[17] Kyvelou, P.; Slack, H.; Mountanou, D. D.; Wadee, M. A.; Britton, T. B.; Buchanan, C.; Gardner, L. (2020) *Mechanical and microstructural testing of wire and arc additively manufactured sheet material* in: Materials & Design 192, 108675.
[18] Laghi, V.; Palermo, M.; Tonelli, L.; Gasparini, G.; Ceschini, L.; Trombetti, T. (2020) *Tensile properties and microstructural features of 304L austenitic stainless steel produced by*

wire-and-arc additive manufacturing in: The International Journal of Advanced Manufacturing Technology 106, 9, pp. 3693–3705.

[19] Feucht, T.; Lange, J.; Waldschmitt, B.; Schudlich, A.-K.; Klein, M.; Oechsner, M. (2020) *Welding Process for the Additive Manufacturing of Cantilevered Components with the WAAM* in: *Advanced Joining Processes*, vol. 125, da Silva, L. F. M.; Martins, P. A. F.; El-Zein, M. S. (eds.), Singapore: Springer, pp. 67–78.

Authors

Prof. Dr.-Ing. Jörg Lange (corresponding author)
j_lange@stahlbau.tu-darmstadt.de
Technical University of Darmstadt
Institute of Steel Construction & Materials Mechanics
Franziska-Braun-Str. 3
64287 Darmstadt, Germany

Thilo Feucht, MSc
feucht@stahlbau.tu-darmstadt.de
Technical University of Darmstadt
Institute of Steel Construction & Materials Mechanics
Franziska-Braun-Str. 3
64287 Darmstadt, Germany

Maren Erven, MSc
erven@stahlbau.tu-darmstadt.de
Technical University of Darmstadt
Institute of Steel Construction & Materials Mechanics
Franziska-Braun-Str. 3
64287 Darmstadt, Germany

How to Cite this Paper

Lange, J.; Feucht, T.; Erven, M. (2020) *3D printing with steel - Additive Manufacturing for connections and structures.* Steel Construction 13, No. 3, pp. 144–153.
https://doi.org/10.1002/stco.202000031

This paper has been peer reviewed. Submitted: 24. April 2020; accepted: 19. June 2020.